JACS
JOURNAL OF THE AMERICAN CHEMICAL SOCIETY
Article
pubs.acs.org/JACS

Cancer Cell Death Induced by the Intracellular Self-Assembly of an Enzyme-Responsive Supramolecular Gelator

Akiko Tanaka,[†] Yuki Fukuoka,[†] Yuka Morimoto,[†] Takafumi Honjo,[†] Daisuke Koda,[‡] Masahiro Goto,[‡] and Tatsuo Maruyama*[,†]

[†]Department of Chemical Science and Engineering, Graduate School of Engineering, Kobe University, 1-1 Rokkodai, Nada-ku, Kobe 657-8501, Japan

[‡]Department of Applied Chemistry, Graduate School of Engineering and Center for Future Chemistry, Kyushu University, 744 Moto-oka, Fukuoka 819-0395, Japan

Supporting Information

ABSTRACT: We report cancer cell death initiated by the intracellular molecular self-assembly of a peptide lipid, which was derived from a gelator precursor. The gelator precursor was designed to form nanofibers via molecular self-assembly, after cleavage by a cancer-related enzyme (matrix metalloproteinase-7, MMP-7), leading to hydrogelation. The gelator precursor exhibited remarkable cytotoxicity to five different cancer cell lines, while the precursor exhibited low cytotoxicity to normal cells. Cancer cells secrete excessive amounts of MMP-7, which converted the precursor into a supramolecular gelator prior to its uptake by the cells. Once inside the cells, the supramolecular gelator formed a gel via molecular self-assembly, exerting vital stress on the cancer cells. The present study thus describes a new drug where molecular self-assembly acts as the mechanism of cytotoxicity.

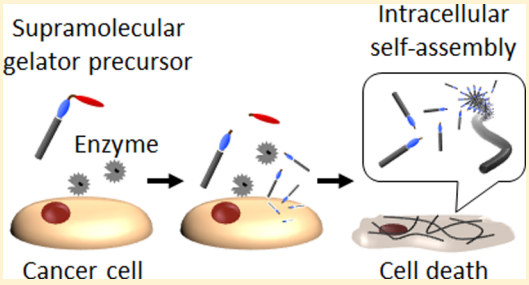

INTRODUCTION

Improving the effectiveness of anticancer drugs, while minimizing their side effects, is a significant challenge for cancer research. To date, various synthetic and naturally derived drugs have been investigated for use in practical cancer therapies. Clinically available anticancer drugs are classified into several types based on their mode of action.[1] These modes of action include inducing the alkylation of DNA, inhibiting specific enzyme activity, preventing microtubule function, inhibiting translation of genetic information, among others. However, most of these drugs damage normal cells as well as cancer cells, often resulting in toxic side effects. Anticancer drugs that are selective to cancer cells and not toxic to normal cells are therefore in high demand. In 2000s, molecularly targeted drugs were approved and highly expected as novel and molecularly effective antitumor drugs.[2] They are classified into the types of small molecules and monoclonal antibodies. They inhibit the molecules related to cancer cell-growth and have fewer side effects than conventional chemotherapy. However, their administrations sometimes cause mutation or a conformational change of a target protein. The resultant resistance to the molecularly targeted drugs becomes a new problem.

Self-assembly plays a significant role in many naturally occurring processes and offers a broad spectrum of approaches for designing and synthesizing artificial functional materials.[3] Molecular self-assembly, in particular, allows us to create functional nanostructures whose performance sometimes surpasses that of the natural systems that they may mimic. Some of oligopeptides and organic compounds can self-assemble into nanofibers or ultrathin films,[4] whose three-dimensional entanglement induces the gelation of solvents; these are known as supramolecular gelators.[5] Functional hydrogels, produced by the supramolecular gelators, have been proposed for many applications including tissue engineering[6] and microarrays for screening physiologically active compounds[7] and to promote wound healing.[8] Xu et al. reported pioneering work that synthetic organic molecules, which penetrated cell membranes and self-assembled to construct nanostructures inside the living cells, significantly affected cellular function.[9]

Here we report a supramolecular gelator whose intracellular molecular self-assembly, triggered by a cancer-related enzyme, causes critical damage to cancer cells while avoiding harm to normal cells. We tested the gelator with the enzyme matrix metalloproteinase-7 (MMP-7), which is excessively produced and secreted by various cancer cells.[10] We designed a precursor peptide-lipid that would produce a supramolecular gelator on enzymatic reaction.[11] The peptide-lipid precursor was hydrolyzed by MMP-7, and the resultant supramolecular gelator was taken up by living cancer cells. Once inside the cells, the supramolecular gelator molecules self-assembled to form nanofibers that critically impaired cellular function and thus killed the cancer cells (Scheme 1a). We demonstrate herein that the intracellular self-assembly of the supramolecular gelator successfully caused selective cancer cell death.

Received: October 2, 2014
Published: December 18, 2014

DOI: 10.1021/ja510156v
J. Am. Chem. Soc. 2015, 137, 770−775

Scheme 1. (a) Cancer Cell Death Induced by Molecular Self-Assembly of an Enzyme-Responsive Supramolecular Gelator and (b) Molecular Structures of *N*-palmitoyl-Gly-Gly-Gly-His-Gly-Pro-Leu-Gly-Leu-Ala-Arg-Lys-$CONH_2$ (ER-C16), *N*-palmitoyl-Gly-Gly-Gly-His-Gly-Pro-Leu-Gly (G-C16), and Leu-Ala-Arg-Lys-$CONH_2$ (Peptide Fragment)

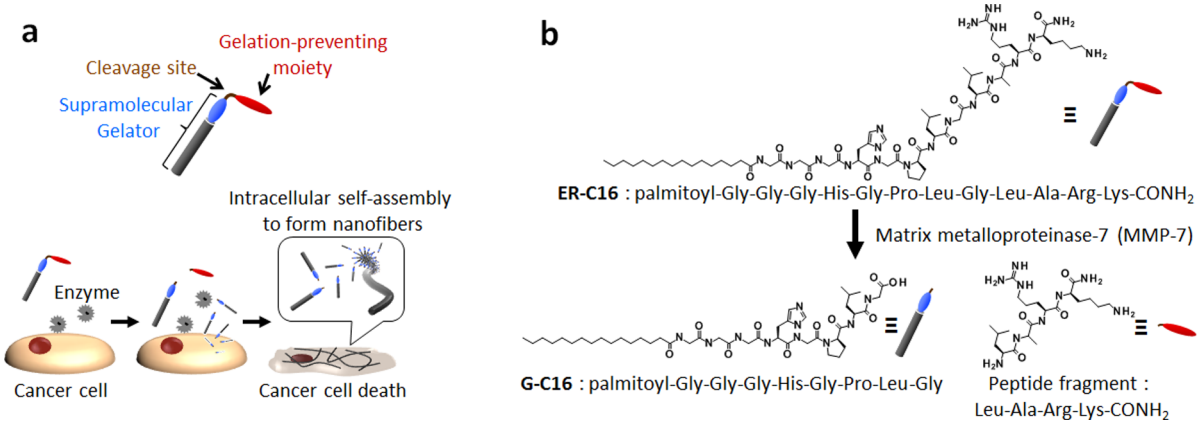

RESULTS AND DISCUSSION

Synthesis and Characterization of the Precursor (ER-C16) of the Supramolecular Gelator (G-C16). To satisfy the design criteria illustrated in Scheme 1a, we designed and synthesized the supramolecular gelator precursor **ER-C16** (*N*-palmitoyl-Gly-Gly-Gly-His-Gly-Pro-Leu-Gly-Leu-Ala-Arg-Lys-$CONH_2$, Scheme 1b). **ER-C16** contained the following four distinct motifs: (1) the 16-carbon alkyl chain to enhance the self-assembly in aqueous solution by providing hydrophobic interactions; (2) the tetrapeptide segment (Gly-Gly-Gly-His), following the alkyl chain, as the major building block because of its ability to act as both an acceptor and a donor of hydrogen bonds;[11] (3) the peptide sequence (Pro-Leu-Gly-Leu), whose cleavage by MMP-7 confers on the molecule the ability to self-assemble, leading to gelation; and (4) the cationic peptide (Arg-Lys), which prevents **ER-C16** from forming nanofibers without having first undergone enzymatic hydrolysis. **ER-C16** and its derivatives were synthesized by peptide solid-phase synthesis using 9-fluorenylmethoxycarbonyl (Fmoc) chemistry.

To characterize the self-assembly properties of **ER-C16**, we first verified that MMP-7 was able to convert **ER-C16** to a supramolecular gelator (**G-C16**, Scheme 1b), which would then be able to self-assemble into nanofibers and induce hydrogelation. MMP-7 (2 μg/mL, final concentration) was added to a 0.2 wt % **ER-C16** solution (50 mM Tris-HCl, 150 mM NaCl, 2 mM $CaCl_2$, pH 7.4), and the solution was kept at 25 °C, resulting in a translucent hydrogel within 2 h. We characterized the morphologies formed by **ER-C16** using a transmission electron microscope (TEM). Figure 1a,b shows the TEM images of the **ER-C16** solution and the gel formed by the addition of MMP-7. While micelle-like morphology was observed before the MMP-7 addition, bundled nanofibers were observed after the addition, which would contribute to the hydrogelation. Differential scanning calorimetry revealed that the hydrogel had a gel−sol transition at about 74 °C (Figure S1). It should be noted that MMP-7 converted more than 50% of the **ER-C16** to **G-C16**.[11] This means that the hydrogel comprised a co-assembled mixture of **G-C16** and **ER-C16**. Indeed, an appropriate mixture of **ER-C16** and **G-C16** formed a hydrogel within 1 h (Figure S2).

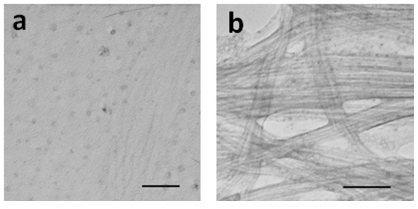

Figure 1. TEM images of the cryo-dried 0.2 wt % **ER-C16** solution (a) and hydrogel (b) obtained after adding MMP-7 (2 μg/mL) to the solution. An aqueous solution was 50 mM Tris-HCl buffer containing 150 mM NaCl and 2 mM $CaCl_2$ (pH 7.4). Both were stained with 2.0 wt % phosphotungstic acid. Scale bars represent 50 and 100 nm, respectively.

The addition of 6 M guanidine hydrochloride or 8 M urea to the gels (prepared with **G-C16** and with **ER-C16** and **G-C16**) caused the dissociation of gel to produce a sol-state, which indicates the significance of hydrogen bonds and hydrophobic interactions among **G-C16** and **ER-C16** molecules in the present gelation.

Using a MMP-7 assay kit, we confirmed that HeLa cells secreted MMP-7 and that the supernatant of the culture medium contained 2.0 μg/mL MMP-7. To evaluate whether MMP-7 secreted by HeLa cells could convert **ER-C16** to **G-C16**, the supernatant from cultured HeLa cells was subjected to the gelation test. After an **ER-C16** solution (200 μL, 3.6 wt %) was added to the supernatant (1 mL) and incubated for 2 days, hydrogelation of the supernatant was observed (Figure S3a). Matrix-assisted laser desorption/ionization time-of-flight mass spectrometry (MALDI-TOF/MS) of the supernatant demonstrated the presence of **G-C16** derived from **ER-C16** (Figure S3b). These results revealed that MMP-7, secreted by HeLa cells, catalyzed the hydrolysis of **ER-C16** at a specific position of the peptide sequence to form **G-C16**, whose molecular self-assembly triggered hydrogelation.

Cytotoxicity to Various Kinds of Cells. The cytotoxicity of **ER-C16** and its derivatives was examined, using HeLa cells as a model for human cancer cells and normal human dermal microvascular endothelial cells (abbreviated MvE cells) as a model for normal human cells. Figure 2a−e shows the results of live/dead assays using calcein AM and ethidium homodimer, in which living cells are dyed green by the intracellular enzymatic hydrolysis of calcein AM and dead cells are dyed red by the intercalation of ethidium homodimer to DNA.[12] Both **ER-C16** (0.02 wt %) and **G-C16** (0.02 wt %) evidently induced the death of HeLa cells (Figure 2a,c). In contrast, MvE cells were alive in the presence of **ER-C16** but killed in the presence of **G-**

DOI: 10.1021/ja510156v
J. Am. Chem. Soc. 2015, 137, 770−775

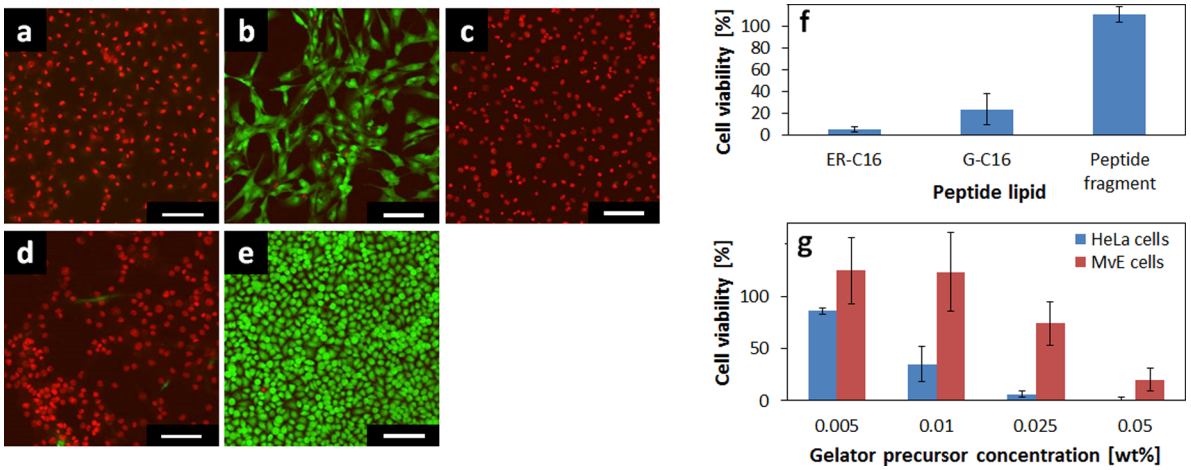

Figure 2. (a–g) Live/dead assays of HeLa cells (a, c, e) and MvE cells (b, d) after incubation for 18 h with **ER-C16** and its derivatives. Cells cultured on a microplate were observed using a confocal laser scanning microscope (CLSM). (a, b) The gelator precursor (**ER-C16**, 0.02 wt %), (c, d) the gelator (**G-C16**, 0.02 wt %), and (e) the peptide fragment (Leu-Ala-Arg-Lys-$CONH_2$, 0.02 wt %). Scale bars represent 100 μm. (f, g) Viability assay (modified MTT assay) of HeLa cells and MvE cells after the incubation for 18 h with **ER-C16** and its derivatives. (f) Effect of peptide lipids and a peptide (0.025 wt %) on the viability of HeLa cells. (g) Effect of **ER-C16** concentration on the cell viability. MvE cells represent primary normal human dermal microvascular endothelial cells. Error bars represent standard deviations in 6 replicates for each sample.

C16 (Figure 2b,d). As mentioned above, **ER-C16** is hydrolyzed by MMP-7 to produce **G-C16** and a peptide fragment (Leu-Ala-Arg-Lys-$CONH_2$). The live/dead assays for the peptide fragment show that HeLa cells were not killed by the peptide fragment (Figure 2e). These results indicated that **ER-C16** had a critical damage to HeLa cells but not to MvE cells and that **G-C16**, the product of hydrolysis of **ER-C16**, was cytotoxic for both kinds of cells.

To quantitatively evaluate the cell viability in the presence of **ER-C16** and its derivatives, viability assays were carried out using Cell Counting Kit-8 (Dojindo, Kumamoto, Japan), which is a modified version of the MTT assay using a highly water-soluble tetrazolium salt.[13] The addition of **ER-C16** and **G-C16** resulted in <5.3% and <24% viability of HeLa cells, respectively (Figure 2f). The peptide fragment (Leu-Ala-Arg-Lys-$CONH_2$) did not exhibit cytotoxicity for the cells. The effect of exposure time on the viability of HeLa cells was also investigated (Figure S4a). In the presence of **ER-C16**, the cell viability fell to 27% after 0.5 h and <17% after only 1.5 h. This result indicates that the cell-killing process was relatively rapid. In the presence of **G-C16**, the cell viability also decreased with time (Figure S4b). Interestingly, the decrease rate of the viability was much slower than that of **ER-C16**. After 4 h, the viability with **G-C16** was still more than 20%, while that with **ER-C16** was almost zero. The possible reason for the difference in the viability would be attributed to the state of the gelator in solution and also to the gelator uptake by the cells. Our previous report and Figure 1 suggest that **ER-C16** was supposed to be present in a micelle-like form and that **G-C16** was supposed to be present in a long nanofiber form.[11] The long nanofiber form might impede the uptake of the gelator molecules by the cells.

Figure S5 also shows time courses of the hydrolysis of **ER-C16** (0.025 wt %) monitored by HPLC. In the case of the hydrolysis by commercial MMP-7 (2 μg/mL), **ER-C16** decreased with time, and more than half of **ER-C16** was hydrolyzed within 1.5 h. In the culture medium of HeLa cells, the time course of the **ER-C16** hydrolysis was very similar to that of commercial MMP-7. As shown in Figure S2, the mixture of **G-C16** (more than 50%) and **ER-C16** co-assembled and formed gel. The hydrolysis of the **ER-C16** coincided with the cell death observed in Figure S4a.

We then investigated the effects of the **ER-C16** concentration on the cell viability (Figure 2g). At 0.005 wt %, **ER-C16** did not affect the viability of HeLa cells and MvE cells. At 0.01 wt %, the viability of HeLa cells drastically decreased to 35%, but that of MvE cells was not affected. At 0.025 wt %, more than 94% of HeLa cells were killed, while only 26% of MvE cells were killed. At 0.05 wt %, most of the HeLa cells and more than 80% of MvE cells were killed; this may be because normal cells also produce and secrete small amounts of MMP-7. The **ER-C16** concentration strongly affected the cell viability and there was a large difference in the viability between the two kinds of cells.

To test our hypothesis that the cytotoxicity of **ER-C16** was triggered by its hydrolysis, catalyzed by MMP-7, we examined the viability of various cancer cells and normal cell types on exposure to **ER-C16**. Figure 3a reveals that **ER-C16** exhibited varying degrees of cytotoxicity to all the tested types of cancer cells, while having a small effect on the two kinds of normal cells (MvE cells and primary human pancreatic epithelial cells (PE cells)).

We anticipated that the cytotoxicity of **ER-C16** was correlated to the amount of MMP-7 secreted by cells. To confirm this relationship, we used a MMP-7 assay kit (SensoLyte 520, AnaSpec, Fremont, CA) to determine the MMP-7 concentration in the culture medium. Figure 3b shows that cancer cells secreted significantly more MMP-7 compared with normal cells (MvE cells and PE cells). For example, HeLa cells, whose viability was remarkably affected by **ER-C16**, secreted a relatively large amount of MMP-7 among the 5 cancer cell lines, and the MMP-7 concentration in the culture medium was 2.0 μg/mL, which was 6 times higher than that of MvE cells. These findings support our hypothesis that the cancer cell death is correlated to the production of **G-C16** by enzymatic hydrolysis of **ER-C16** and that the amount of **G-C16** is correlated to the cytotoxicity.

HeLa cells and MvE cells were cocultured using a coculture system (micro-Insert 4well, ibidi GmbH, Planegg, Germany)[14] to evaluate the selective cytotoxicity of **ER-C16** to cancer cells.

DOI: 10.1021/ja510156v
J. Am. Chem. Soc. 2015, 137, 770–775

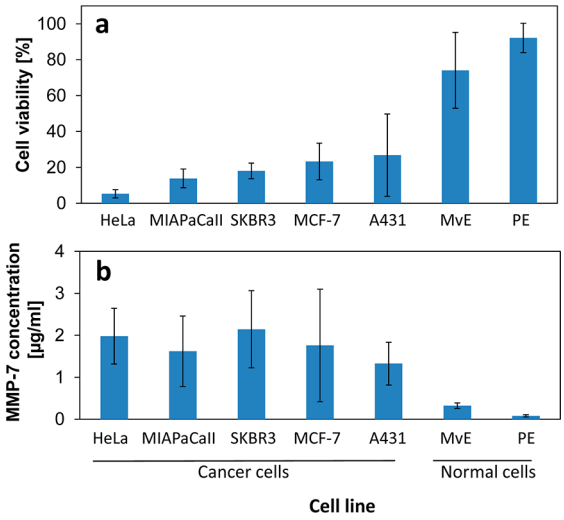

Figure 3. (a) Viability assays of cancer cells and normal human cells after incubation with **ER-C16** (0.025 wt %). (b) MMP-7 concentration in the culture media after culturing the cells. PE represents primary human pancreatic epithelial cells.

Figure 4 shows the live/dead assays for HeLa cells and MvE cells 18 h after the addition of **ER-C16** (0.02 wt %). More than

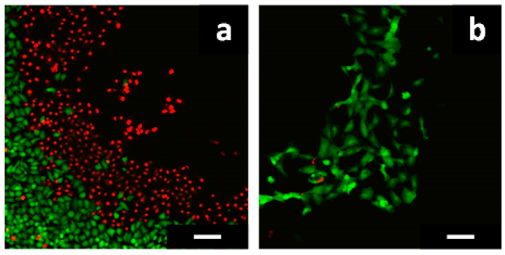

Figure 4. Live/dead assays of HeLa cells (a) and MvE cells (b) using CLSM and a coculture system. CLSM observation was performed after incubation with **ER-C16** (0.02 wt %) for 37 °C for 18 h. Scale bars represent 100 μm.

half of HeLa cells (Figure 4a) were dyed red (dead) and most of the MvE cells (Figure 4b) were dyed green (alive), meaning the cytotoxicity of **ER-C16** was selective to HeLa cells.

Mechanism Leading to Cancer Cell Death. To verify our hypothesis regarding the cell-killing mechanism of **ER-C16**, we synthesized three types of peptide lipids as analogues of **ER-C16** (Figure 5a). The shorter hydrophobic tail of **ER-C12**, having 12 carbons instead of 16 carbons, conferred on this molecule less of the hydrophobic interaction that is required for its self-assembly (hydrogelation) in an aqueous environment.[15] **NR-1** and **NR-2** differed in their peptide sequences, designed not to be hydrolyzed by MMP-7 but rather to maintain intermolecular electrostatic repulsion via their cationic or anionic amino acid residues. Indeed, while they were soluble in an aqueous buffer similar to **ER-C16**, they did not induce hydrogelation in the presence of MMP-7. The live/dead assays of HeLa cells revealed that these peptide lipids did not induce the death of HeLa cells (Figure 5b–d). The viability assays also showed negligible or remarkably reduced cytotoxicity of these peptide lipids to HeLa cells (Figure 5e). These results suggested that molecular self-assembly of the supramolecular gelator inside or outside cells played a key role in killing cells and that the introduction of enzyme responsiveness to the

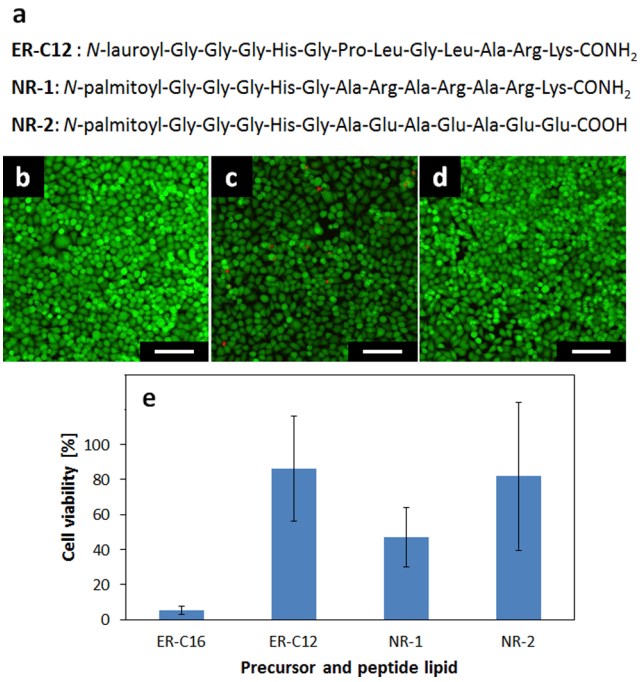

Figure 5. (a) Molecular structures of peptide lipids (**ER-C12**, **NR-1**, and **NR-2**) as analogues of **ER-C16**. (b–d) Live/dead assays of HeLa cells using the analogues (0.02 wt % each) by CLSM: (b) **ER-C12**, (c) **NR-1**, and (d) **NR-2**. Scale bars represent 100 μm. (e) Viability assay of HeLa cells after the incubation with the analogues (0.025 wt %) for 37 °C for 18 h.

supramolecular gelator achieved cytotoxicity selective to cancer cells.

NR-1 resulted in relatively reduced viability. MALDI-TOF/MS analysis of treated HeLa cells revealed the partial hydrolysis of **NR-1** at different peptide bonds to produce small amounts of palmitoyl-Gly-Gly-Gly-His-Gly-Ala-Arg-Ala-Arg-Ala and palmitoyl-Gly-Gly-Gly-His-Gly-Ala-Arg-Ala. Since no hydrolysis of **NR-1** by commercial MMP-7 was confirmed, the hydrolysis of **NR-1** was probably due to other proteolytic enzymes in a culture medium or inside a cell. This would account for the relatively reduced viability in **NR-1**.

To obtain further information how the self-assembly and hydrogelation causes the death of cancer cells, fluorescence recovery after photobleaching was performed. HeLa cells incubated with **G-C16** and a **G-C16** analogue having a fluorophore (7-nitrobenzo-2-oxa-1,3-diazole, NBD) at the end of its alkyl chain (**NBD-G-C12**, Figure 6a). The structural homology between **G-C16** and **NBD-G-C12** allowed these molecules to form nanofibers via co-assembly with each other and allowed the fluorescent visualization of the self-assembly in microscope observation (Figure S6).[5f] The self-assembly of **G-C16** inside HeLa cells was successfully visualized using **NBD-G-C12** (Figure 6b), suggesting the uptake of **G-C16** by HeLa cells. We then photobleached the small area indicated by a white circle in Figure 6b. The fluorescence did not recover 40 min after photobleaching (Figure 6c,d). This result was attributed to the high viscosity inside the cell, implying intracellular hydrogelation by **G-C16**. Kuimova et al. recently reported the strong relationship between cell death and high intracellular viscosity.[16] Our findings and the literature suggest that intracellular hydrogelation by the supramolecular gelator may indeed have caused cell death in the present study.

DOI: 10.1021/ja510156v
J. Am. Chem. Soc. 2015, 137, 770–775

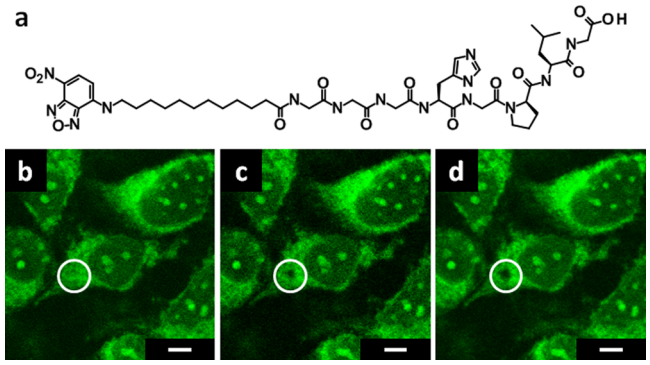

Figure 6. (a) Molecular structure of **NBD-G-C12**. (b–d) Fluorescence recovery after photobleaching of HeLa cells observed using CLSM. HeLa cells were incubated with **G-C16** (0.05 wt %) and dyed with **NBD-G-C12** (5.0×10^{-4} wt %) for 18 h. A white circle indicates the photobleaching region. (b) Before photobleaching, (c) just after photobleaching, and (d) 40 min after photobleaching. Scale bars represent 5 μm.

To further explore the intracellular hydrogelation, we collected the dead HeLa cells and broke the cells by ultrasonication. The cell lysate formed a hydrogel (Figure 7a)

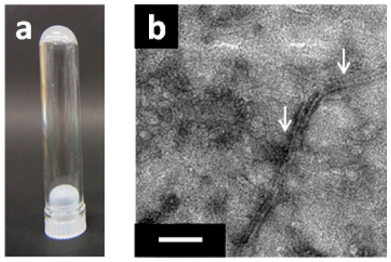

Figure 7. (a) Gelation test (inverted test tube) of the lysate of HeLa cells that were killed by **ER-C16**. (b) TEM observation of the lysate of the dead HeLa cells. Scale bars represent 100 nm.

and exhibited a thermoreversible gel–sol transition. MALDI-TOF/MS analysis (Figure S7) revealed the presence of **G-C16** in the cell lysate, similar to what is evident in Figure S3b. This analysis also demonstrates the presence of both **G-C16** and **ER-C16** in the cell lysate, implying the molecular co-assembly of **G-C16** and **ER-C16** inside the cells. Furthermore, TEM observation (Figure 7b) of the hydrogel revealed bundled nanofibers, indicated by arrows, approximately 10 nm in width and several micrometers in length, which are morphologically very similar to the nanofibers formed by **G-C16** in aqueous solution (Figure 1b). It should be noted that the cell lysate of living HeLa cells without **ER-C16** did not form a hydrogel and that the lysate did not contain long nanofibers visible by TEM observation. These results support our hypothesis that the cell death was induced by the intracellular formation and subsequent hydrogelation of **G-C16** nanofibers.

CONCLUSIONS

Here we propose the enzyme-triggered molecular self-assembly of a low-molecular-weight gelator for novel anticancer applications. Its precursor (**ER-C16**) exhibited remarkable cytotoxicity to several cancer cell lines, and low cytotoxicity to normal cells. Coculture of the cancer cells and normal cells, and exposure of this sample to **ER-C16**, confirmed that the cytotoxicity of **ER-C16** was selective to cancer cells. The cytotoxicity was proportional to the amount of MMP-7 secreted specifically from cancer cells. The mechanism of **ER-C16** cytotoxicity relies on its hydrolysis by MMP-7, yielding the supramolecular gelator (**G-C16**) whose self-assembly exerts vital stress on the cancer cells. Due to the unique cytotoxic mechanism, cancer cells will be unlikely to acquire resistance to the present strategy comparing to conventional cytotoxic chemotherapy and molecularly targeted therapy.

Because self-assembly can amplify a molecular-level event inside or outside a cell, it holds great promise for therapeutic applications.[15,17] Many diseases start via molecular malfunctions on a scale that is too small to detect by present diagnostic techniques. Appropriately designed self-assembled systems could target other diseases or toxic bacteria. Indeed, Wells et al. reported that self-assembly of their synthesized small molecules formed a complex that could bind to procaspase-3 and stimulate the apoptosis cascade.[18] Fukushima et al. also reported strong antifungal activity of a supramolecular self-assembled system.[19] We predict that molecular self-assembly will soon be more widely used to create novel bioactive materials for therapeutics.[20]

EXPERIMENTAL SECTION

Solid-Phase Synthesis of N-Acylated Peptides. N-Acylated peptides were prepared by the standard 9-fluorenylmethoxycarbonyl solid-phase peptide synthesis on a 0.3 mmol scale. Details are in the Supporting Information.

Cells Culturing. Frozen cells were harvested by rapid thawing in a 37 °C water bath and were washed with fresh culture medium. Details of the culture medium are summarized in Table S1. The medium was exchanged two times per week. The cell cultures were maintained at 37 °C and 5% CO_2.

Live/Dead Assay. Cell survival after exposure to the gelator precursor was evaluated using the live/dead viability/cytotoxicity kit (Invitrogen, Carlsbad, CA). Samples were processed according to the manufacturer's instructions. Briefly, after allowing the cells to adhere, 1.0×10^5 cells/1 mL in a 24-well microplate were incubated with **ER-C16** or **G-C16** at 37 °C for 18 h. Cells were stained with the live/dead assay reagents (calcein AM and ethidium homodimer) and then incubated at 37 °C for 20 min. After washing with warm 1 mL phosphate-buffered saline (PBS), cells were observed by confocal laser scanning microscopy (CLSM; Fluoview FL1000, Olympus, Tokyo, Japan). Living cells exhibited green fluorescence, and dead cells exhibited red fluorescence.

In Vitro Cell Viability. Cytotoxicity of **ER-C16** was evaluated using Cell Counting Kit-8 (Dojindo) in accordance with the manufacturer's instructions. Briefly, cells were plated 5.0×10^3 cells/100 μL in a 96-well plate and incubated for 24 h at 37 °C. The cells were treated with the gelator precursor (or other peptide lipids, as controls) at varying concentrations and incubated at 37 °C for 18 h. Then 10 μL of a Cell Counting Kit-8 solution was added to each well. After incubation for 1 h, the absorbance at 450 nm was measured using a microplate reader (ARVOsx 1420 multilabel counter, PerkinElmer, Waltham, MA) at 25 °C. The assay was performed in five replicates for each sample.

MMP-7 Activity Measurements. MMP-7 activity was determined using a Sensolyte 520 MMP-7 Assay Kit Fluorimetric (AnaSpec, Fremont, CA) according to the manufacturer's instructions. Briefly, supernatants of cell culture media were collected after incubation for 24 h and were centrifuged for 15 min at 1000 × *g*, 4 °C. The cell culture supernatants (50 μL) were then incubated with the FAM/QXL 520 fluorescence resonance energy transfer substrate solution (50 μL) for 40 min in a black 96-well plate at 37 °C in the dark. After adding the stop solution (50 μL), fluorescent measurements were performed using a microplate reader with excitation at 490 nm and emission at 520 nm. Commercially available MMP-7 (Prospec, East Brunswick,

DOI: 10.1021/ja510156v
J. Am. Chem. Soc. 2015, 137, 770–775

NJ) was used as a positive control. The activity measurement was performed in five replicates for each sample.

Fluorescence Recovery after Photobleaching (FRAP). After allowing HeLa cells to adhere, 4.0×10^5 cells/2 mL in 35 mm/glass base dish were incubated with **G-C16** (0.05 wt %) and **NBD-G-C12** (5.0×10^{-4} wt %) at 37 °C for 18 h. After washing with warm 1 mL PBS, cells were then observed by CLSM.

Coculture of HeLa and MvE Cells. HeLa cells and MvE cells were cocultured using a micro-Insert 4well (ibidi GmbH, Planegg, Germany) to evaluate the cytotoxicity of **ER-C16**. A complete medium kit with serum and cultureboost-R (a mixture of human recombinant growth factors and porcine heparin) was used as a culture medium. Each kind of cell was plated 5.0×10^2 cells/8 μL in a microwell of a micro-Insert 4well dish. The supernatants were removed and replaced with 150 μL of a culture medium containing **ER-C16** (0.02 wt %), following which the cells were incubated for 37 °C for 18 h. Cells were then stained with the live/dead assay reagents (calcein AM and ethidium homodimer) and incubated at 37 °C for 20 min. After washing with warm 150 μL PBS, cells were observed by CLSM.

Gelation Tests of Cell Lysate. After allowing HeLa cells to adhere, 1.0×10^6 cells/10 mL in a 100 mm/tissue culture dish were incubated with **ER-C16** (0.025 wt %) at 37 °C for 18 h. After collecting the cells by trypsin treatment, HeLa cells were washed by PBS. The HeLa cells collected were homogenized using an ultrasonic homogenizer and freeze-dried. The lysate of HeLa cells was dissolved in 50 mM phosphate buffer (pH 7.4), whose weight was equal to that of the water evaporated in the freeze-drying, in a glass microtube by heating and by slowly cooling down to room temperature to form hydrogel.

TEM observation was performed using a JEOL JEM2100F microscope (JEOL Ltd., Tokyo, Japan). A piece of the cell lysate (stained with 2.0 wt % phosphotungstic acid) was placed on a hydrophilic butyral-coated copper grid and dried for 12 h under vacuum. The grid was observed using an acceleration voltage of 200 kV.

■ ASSOCIATED CONTENT

Supporting Information

Materials, instruments, synthesis, and characterization of compounds, experimental procedures, and figures. This material is available free of charge via the Internet at http://pubs.acs.org.

■ AUTHOR INFORMATION

Corresponding Author

tmarutcm@crystal.kobe-u.ac.jp

Notes

The authors declare no competing financial interest.

■ ACKNOWLEDGMENTS

We thank Prof. A. Kondo, Prof. T. Takeuchi, and Prof. H. Matsuyama for their technical help. We thank Prof. A. Kondo for kindly providing cancer cells. This work was supported partially by Special Coordination Funds for Promoting Science and Technology, Creation of Innovation Centers for Advanced Interdisciplinary Research Areas (Innovative Bioproduction Kobe), MEXT, Japan, by JSPS KAKENHI grant no. 25630380, by Takeda Science Foundation, and also by Astellas Foundation for Research on Metabolic Disorders.

■ REFERENCES

(1) Avendaño, C.; Menéndez, J. C. *Medicinal chemistry of anticancer drugs*, 1st ed.; Elsevier: Amsterdam, 2008; pp xv, 442.

(2) Sebolt-Leopold, J. S.; English, J. M. *Nature* **2006**, *441*, 457−462.

(3) (a) Stupp, S. I.; LeBonheur, V. V.; Walker, K.; Li, L. S.; Huggins, K. E.; Keser, M.; Amstutz, A. *Science* **1997**, *276*, 384−389. (b) Harris, S.; Buchinski, B.; Grzybowski, S.; Janssen, P.; Mitchell, G. W.; Farquharson, D. *Can. Med. Assoc. J.* **2000**, *163*, 1163−1166. (c) Lehn, J. M. *Science* **2002**, *295*, 2400−2403.

(4) (a) Yamada, N.; Ariga, K.; Naito, M.; Matsubara, K.; Koyama, E. *J. Am. Chem. Soc.* **1998**, *120*, 12192−12199. (b) Ariga, K.; Kikuchi, J.; Naito, M.; Koyama, E.; Yamada, N. *Langmuir* **2000**, *16*, 4929−4939.

(5) (a) Hanabusa, K.; Yamada, M.; Kimura, M.; Shirai, H. *Angew. Chem., Int. Ed.* **1996**, *35*, 1949−1951. (b) Murata, K.; Aoki, M.; Nishi, T.; Ikeda, A.; Shinkai, S. *J. Chem. Soc. Chem. Comm.* **1991**, 1715−1718. (c) Kiyonaka, S.; Sugiyasu, K.; Shinkai, S.; Hamachi, I. *J. Am. Chem. Soc.* **2002**, *124*, 10954−10955. (d) Zhang, Y.; Gu, H. W.; Yang, Z. M.; Xu, B. *J. Am. Chem. Soc.* **2003**, *125*, 13680−13681. (e) van Bommel, K. J.; van der Pol, C.; Muizebelt, I.; Friggeri, A.; Heeres, A.; Meetsma, A.; Feringa, B. L.; van Esch, J. *Angew. Chem., Int. Ed.* **2004**, *43*, 1663−1667. (f) Minakuchi, N.; Hoe, K.; Yamaki, D.; Ten-No, S.; Nakashima, K.; Goto, M.; Mizuhata, M.; Maruyama, T. *Langmuir* **2012**, *28*, 9259−9266.

(6) (a) Hartgerink, J. D.; Beniash, E.; Stupp, S. I. *Science* **2001**, *294*, 1684−1688. (b) Holmes, T. C.; de Lacalle, S.; Su, X.; Liu, G.; Rich, A.; Zhang, S. *Proc. Natl. Acad. Sci. U.S.A.* **2000**, *97*, 6728−6733. (c) Silva, G. A.; Czeisler, C.; Niece, K. L.; Beniash, E.; Harrington, D. A.; Kessler, J. A.; Stupp, S. I. *Science* **2004**, *303*, 1352−1355.

(7) (a) Kiyonaka, S.; Sada, K.; Yoshimura, I.; Shinkai, S.; Kato, N.; Hamachi, I. *Nat. Mater.* **2004**, *3*, 58−64. (b) Yoshimura, I.; Miyahara, Y.; Kasagi, N.; Yamane, H.; Ojida, A.; Hamachi, I. *J. Am. Chem. Soc.* **2004**, *126*, 12204−12205.

(8) Yang, Z. M.; Xu, K. M.; Wang, L.; Gu, H. W.; Wei, H.; Zhang, M. J.; Xu, B. *Chem. Commun.* **2005**, 4414−4416.

(9) (a) Yang, Z.; Liang, G.; Guo, Z.; Guo, Z.; Xu, B. *Angew. Chem., Int. Ed.* **2007**, *46*, 8216−8219. (b) Kuang, Y.; Xu, B. *Angew. Chem., Int. Ed.* **2013**, *52*, 6944−6948. (c) Yang, Z. M.; Xu, K. M.; Guo, Z. F.; Guo, Z. H.; Xu, B. *Adv. Mater.* **2007**, *19*, 3152−3156.

(10) (a) Polette, M.; Nawrocki-Raby, B.; Gilles, C.; Clavel, C.; Birembaut, P. *Crit. Rev. Oncol. Hematol.* **2004**, *49*, 179−186. (b) Tanioka, Y.; Yoshida, T.; Yagawa, T.; Saiki, Y.; Takeo, S.; Harada, T.; Okazawa, T.; Yanai, H.; Okita, K. *Br. J. Cancer* **2003**, *89*, 2116−2121.

(11) Koda, D.; Maruyama, T.; Minakuchi, N.; Nakashima, K.; Goto, M. *Chem. Commun.* **2010**, *46*, 979−981.

(12) Papadopoulos, N. G.; Dedoussis, G. V.; Spanakos, G.; Gritzapis, A. D.; Baxevanis, C. N.; Papamichail, M. *J. Immunol. Methods* **1994**, *177*, 101−111.

(13) Ishiyama, M.; Miyazono, Y.; Sasamoto, K.; Ohkura, Y.; Ueno, K. *Talanta* **1997**, *44*, 1299−1305.

(14) Miyanari, Y. *Methods* **2014**, *69*, 198−204.

(15) Roy, S.; Dasgupta, A.; Das, P. K. *Langmuir* **2007**, *23*, 11769−11776.

(16) Kuimova, M. K.; Botchway, S. W.; Parker, A. W.; Balaz, M.; Collins, H. A.; Anderson, H. L.; Suhling, K.; Ogilby, P. R. *Nat. Chem.* **2009**, *1*, 69−73.

(17) Ikeda, M.; Tanida, T.; Yoshii, T.; Kurotani, K.; Onogi, S.; Urayama, K.; Hamachi, I. *Nat. Chem.* **2014**, *6*, 511−518.

(18) Zorn, J. A.; Wille, H.; Wolan, D. W.; Wells, J. A. *J. Am. Chem. Soc.* **2011**, *133*, 19630−19633.

(19) Fukushima, K.; Liu, S.; Wu, H.; Engler, A. C.; Coady, D. J.; Maune, H.; Pitera, J.; Nelson, A.; Wiradharma, N.; Venkataraman, S.; Huang, Y.; Fan, W.; Ying, J. Y.; Yang, Y. Y.; Hedrick, J. L. *Nat. Commun.* **2013**, *4*, 2861.

(20) Niece, K. L.; Hartgerink, J. D.; Donners, J. J. J. M.; Stupp, S. I. *J. Am. Chem. Soc.* **2003**, *125*, 7146−7147.

DOI: 10.1021/ja510156v
J. Am. Chem. Soc. 2015, 137, 770−775